2021 43rd Annual International Conference of the
IEEE Engineering in Medicine & Biology Society (EMBC)
Oct 31 - Nov 4, 2021. Virtual Conference

Basic Graphic Shape Decoding for EEG-based Brain-Computer Interfaces*

Jingjuan Qiao[1], Jiabei Tang[1], Jiajia Yang[1, 2], Minpeng Xu[1, 2], *Member, IEEE*, Dong Ming[1, 2], *Senior Member, IEEE*

***Abstract*—Image decoding using electroencephalogram (EEG) has became a new topic for brain-computer interface (BCI) studies in recent years. Previous studies often tried to decode EEG signals modulated by a picture of complex object. However, it's still unclear how a simple image with different positions and orientations influence the EEG signals. To this end, this study used a same white bar with eight different spatial patterns as visual stimuli. Convolutional neural network (CNN) combined with long short-term memory (LSTM) was employed to decode the corresponding EEG signals. Four subjects were recruited in this study. As a result, the highest binary classification accuracy could reach 97.2%, 95.7%, 90.2%, and 88.3% for the four subjects, respectively. Almost all subjects could achieve more than 70% for 4-class classification. The results demonstrate basic graphic shapes are decodable from EEG signals, which hold promise for image decoding of EEG-based BCIs.**

I. Introduction

A brain-computer interface (BCI) measures the brain activity and converts it into artificial output that can replace, restore, enhance, supplement, or improve a natural neural output [1]. BCIs could provide communication and control channels that do not depend on the brain's normal output peripheral nerves and muscles [2]. With the advantage of noninvasiveness, high temporal resolution and ease of use, electroencephalogram (EEG) is the most welcomed neuroimaging method for BCIs.

The visual perception plays a major role in feeling the outside world, and most of the information perceived by human comes from vision [3]. The visual evoked potentials (VEPs) were utilized by researchers to design a number of BCIs with large instruction set and high interaction speed [4, 5]. However, these systems focused on decoding the point at which the users were staring. The functional magnetic resonance imaging (fMRI) researches have proved that the visual stimulus in the two-dimension space could activate a corresponding pattern in the visual cortex at voxel level, which could be decoded by machine learning [6]. For example, Horikawa et al. reproduced the visual scenes by constructing a voxel-level regression model with the visual features extracted from human fMRI brain activities [7].

* Research supported by the National Natural Science Foundation of China. (81630051, 81925020, 61976152) and Young Elite Scientist Sponsorship Program by China Association for Science and Technology (2018QNRC001). Corresponding author: Jiabei Tang, e-mail: jiahe@tju.edu.cn.

[1] School of Precision Instruments & Optoelectronics Engineering, Tianjin University, Tianjin, 300072 China.

[2] Academy of Medical Engineering and Translational Medicine, Tianjin University, Tianjin, 300072 China.

Some studies have explored the feasibility to decode the pictures of complex object from the visual evoked EEGs. For example, Zheng et al. proposed an automated visual classification framework, and realized classification of EEGs evoked by images [8]. Rashkov et al. introduced a closed-loop system that reconstructed the observed images from the EEGs [9]. However, physiological studies have demonstrated that the activation of primary visual cortex could be influenced by the color, the contrast, and the location etc [10], and most of the above EEG studies used images of real objects (e.g. the ImageNet [11] dataset) as the stimulation, of which the characters were complex and made it difficult to understand the influence of each factor on EEG signals. Therefore, it is necessary to verify the recognizability of EEGs evoked by basic graphic shapes.

This study aimed at classifying EEGs induced by different simple spatial patterns, i.e. ignoring the influence of other image factors, and giving an insight into decoding compound shapes in the future. To this end, a same white bar with eight different spatial patterns was designed as the stimulation, and a model based on convolutional neural network (CNN) and long short-term memory (LSTM) was built for pattern recognition.

II. Methods

A. Experimental Paradigm

The visual stimuli were constituted by the same white bar with different positions or orientations. Each spatial pattern subtended 6° of visual angle, as shown in Fig. 1(A). During the experiment, the subject was asked to focus on the dot at the center of the screen. The square wave stimulation method was used to generate flickers using the PsychoPy.

This study designed eight spatial patterns: Up (horizontal), Middle (horizontal), Down (horizontal), Left (vertical), Middle (vertical), Right (vertical), Oblique 1 (45°), Oblique 2 (135°), as shown in Fig. 1(B). It should be noted that some of these patterns stimulated both the central and lateral visual field, and the central visual field could produce stronger VEPs that might submerge the weak VEPs of the lateral visual field. Hence, a black circle with a radius of 2 cm appeared at the center of the screen to reduce the influence of central VEPs during the experiment.

During the experiment, eight spatial patterns were randomly presented, and flashed at the frequency of 2 Hz. Each trial started with a rest period for 2 s, followed by a task period for 4 s. A checkerboard would appeared for 0.5 s during the rest period, ensuring that brain activities driven by previous pattern were "cleared".

Figure 1. Experimental paradigm. (A) The sketch map of stimulation. (B) Eight kinds of spatial patterns.

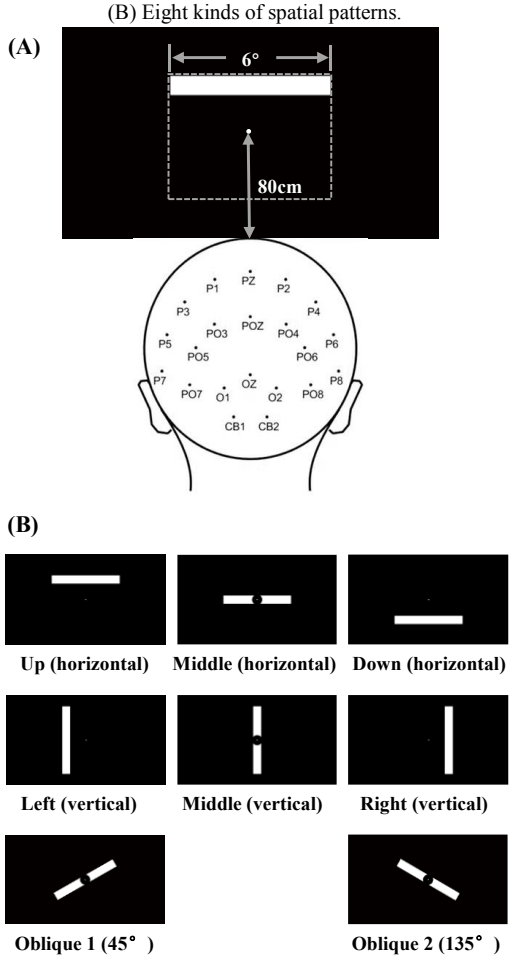

B. Experimental Procedure

Four subjects (one male and three females) aged 22 to 25 years old participated in this study. All subjects had normal or corrected vision. The study was conducted in accordance with the Declaration of Helsinki and the experimental procedures were approved by the Institutional Review Board at Tianjin University. Written consent was obtained from each subject after giving a detailed explanation of the experiment. The subjects were seated at a distance of about 80 cm from a 23-inch liquid-crystal display (LCD) monitor with a refresh rate of 60 Hz and were required to gaze at center of the screen.

In order to meet the data demand for neural network, each subject performed three experiments within a week. Each experiment contained 26 blocks, in which 24 trials with each spatial pattern appearing three times were presented in a random order. The relax time between blocks was determined by the subjects.

C. EEG Recording and Processing

A Neuroscan SynAmps2 amplifier and a 64-Channel Quick-Cap were used during the acquisition process. The Ag/AgCl electrodes of the Quick-Cap were placed at standard positions of international 10-20 system. All channels took the vertex as the reference electrode. The EEG data from twenty-one channels around the occipital area (P7, P5, P3, P1, PZ, P2, P4, P6, P8, PO7, PO5, PO3, POZ, PO4, PO6, PO8, CB1, O1, OZ, O2 and CB2, see Fig. 1(A)) were used for analysis. A 50 Hz notch filter and band-pass filter (0.1~200 Hz) were used during the EEG acquisition, and the sampling frequency was set to 1000 Hz.

In pre-processing, the data were band-pass filtered to 1~70 Hz with an infinite impulse response (IIR) filter and standardized with the z-score method. In this study, each trial was separated into 8 times of flash (2 Hz × 4 s), and the EEG epochs were extracted in [50 ms, 350 ms] according to the onset of the flash, thus generating 24 epochs for each spatial pattern. The classification test was performed with a 10-fold cross-validation method.

D. Feature Analysis and Target Recognition

This research employed a deep learning model based on CNN and LSTM. As one of the representative algorithms of deep learning, CNN is widely used in many fields like computer vision and natural language processing. Generally, CNN includes convolutional layer, batch normalization (BN) layer, activation function, pooling layer and fully connected layer. Convolution can be considered as an effective method to extract features. BN can adjust the input of each layer to a standard normal distribution with a mean value of 0 and a variance of 1, which could solve vanishing gradient problems in the neural network. The features which CNN learns are hierarchical composing high-complexity features out of low-complexity, which was more efficient than learning high-complexity features directly [12].

LSTM is a special kind of recurrent neural networks (RNNs) [13], which was proposed by Hochreiter and Schmidhuber in 1997 [14]. The traditional RNNs extract information from time dimension with cyclic kernel. However, vanishing gradient or gradient explosion problems caused by multi-stage backpropagation make RNN difficult to remember long-term dependencies. LSTM introduced three gates to solve the problem: input gate i_t, forget gate f_t and output gate o_t. The interaction between the gates and inputs are shown in Eqs. (1)-(3):

$$i_t = \sigma\left(W_i \cdot \left[h_{t-1}, x_t\right] + b_i\right) \tag{1}$$

$$f_t = \sigma\left(W_f \cdot \left[h_{t-1}, x_t\right] + b_f\right) \tag{2}$$

$$o_t = \sigma\left(W_o \cdot \left[h_{t-1}, x_t\right] + b_o\right) \tag{3}$$

In the above formulas x_t is the input feature of the current moment, h_{t-1} is the short-term memory of the last moment. W_i, W_f, and W_o are parameter matrices, and b_i, b_f, b_o are bias items. σ is the Sigma activation function, which makes the threshold range between 0 and 1.

By using a gate mechanism to control the circulation and loss of information, LSTM could remember long-term information. It is beneficial for us to analyze long sequences of EEG signals from the time dimension.

In this study, an automated visual classification model based on CNN and LSTM was proposed. The model consisted of a 5-layer convolution network, a 3-layer long-short memory network and one fully connected layer with SoftMax

activation function, as shown in Fig.2. The number of kernel and the kernel size were determined based on the preliminary experiments. In this study, one-dimensional convolution kernels were used to extract features. Batch normalization and dropout were implemented which could lead to faster training of the network as well as better conservation of information throughout the hierarchical process, and avoid overfitting of the network based on their nature [12]. The batch normalization was performed after the third and fifth layers of convolution, which also solved vanishing gradient problems by transforming the input of each layer into a standard normal distribution with a mean value of 0 and a variance of 1. The 50% dropout was carried out after the first batch normalization and the third LSTM layer. The size of batch was set as 128.

Figure 2. The visual classification model based on CNN and LSTM

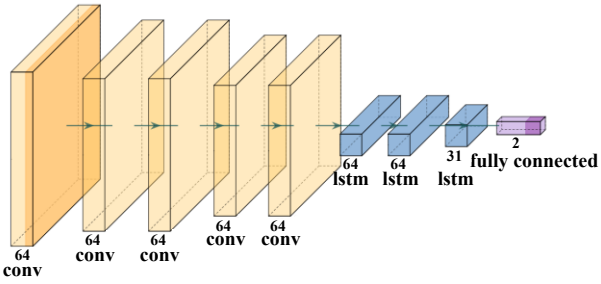

As an important parameter in deep learning, the learning rate controlled the optimization speed and determined whether the network can reach the optimal model. Excessive large or small learning rate would lead to non-convergence or local optimum of the model. To this end, a fixed step decay strategy was adopted to adjust the learning rate. After N epochs, the learning rate became half of the original, where N was adjusted according to different data sets.

The eight spatial patterns described in the experimental paradigm were respectively numbered 1~8, of which 2, 5, 7, 8 were displayed at the center of the screen, and 1, 3, 4, 6 were displayed around the screen. It can be seen that 2, 5, 7, 8 had different orientations (0°, 90°, 45°, 135°), and 1, 3, 4, 6 had different positions (up, down, left, right). In order to explore the specific response of EEGs to different spatial patterns, eight targets were first combined in pairs, and divided into three groups. Group A: both the two targets contain the central vision field (2 vs. 5, 2 vs. 7, 2 vs. 8, 5 vs. 7, 5 vs. 8, 7 vs. 8). Group B: one of the two targets contain the central vision field (2 vs. 1, 2 vs. 3, 2 vs. 4, 2 vs. 6, 5 vs. 1, 5 vs. 3, 5 vs. 4, 5 vs. 6, 7 vs. 1, 7 vs. 3, 7 vs. 4, 7 vs. 6, 8 vs. 1, 8 vs. 3, 8 vs. 4, 8 vs. 6). Group C: neither target contains a central vision field (1 vs. 3, 1 vs. 4, 1 vs. 6, 3 vs. 4, 3 vs. 6, 4 vs. 6).

To better evaluate the performance of the BCI system, four, six, and eight targets were selected from eight spatial patterns in turn for verification. Since there are C_8^4=70 combinations of four different targets, and C_8^6=28 combinations of six different targets, which will greatly increase the time of testing, only part of the combinations were selected based on the results of binary classification.

In order to further verify the separability of EEGs induced by basic graphic shapes, a visualization method of pixel-wise input attribution called layer-wise relevance propagation (LRP) which has been used in understanding the internal representation and decision processes of the networks was adopted. Specifically, the layer of LSTM was visualized and the relevance maps of 500 trials were averaged. Meanwhile, the data were down-sampled to 500Hz to get better visualization effects.

III. Results And Analysis

A. The average accuracy of binary classification

Fig. 3 shows the average accuracies of each subject for group A, group B, and group C. As can be seen, the average accuracies of group B were 93.8%, 88.6%, 84.8%, and 83.9%, respectively. The correct recognition of basic graphic shapes meant that the proposed BCIs system could distinguish the EEGs evoked by the basic elements, which was in line with the transmission mechanism of visual information [15].

Figure 3. The average correct rate of each subject in group A, group B, and group C.

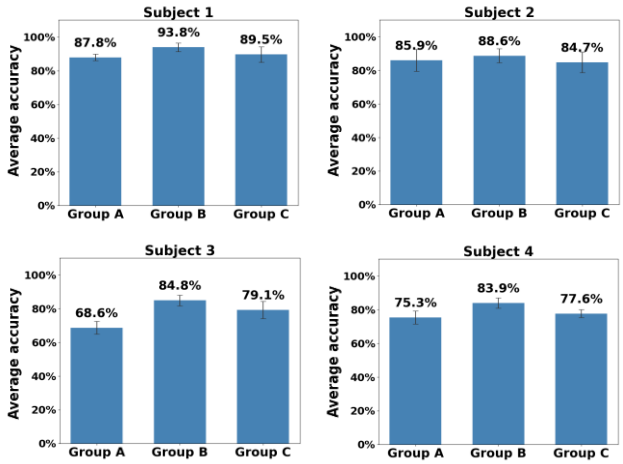

In addition, it could be seen that the average accuracies of group B among the four subjects were higher than those of group A and group C, which showed that there is a greater difference between EEGs evoked by the central and lateral visual field. Besides, Group A had the lowest average accuracies among the three groups except for subject 2. This might be due to the fact that the stimulus at the central visual field could elicit stronger VEPs than that at the peripheral visual field [16]. Although there was a black circle at the center of the screen in this study, the interference caused by the central visual field had not been completely eliminated, the performance of the classifier to discriminate the weak peripheral VEPs evoked by different orientations might be degraded. Further experiment needs to be designed to verify the above conjecture.

B. Performance of multiple classes recognition

Fig. 4 displays the recognition accuracies of different number of targets with the proposed model. The spatial pattern combinations with the highest accuracy were selected for each subject considering the individual differences.

Table 1. Selected combinations of each subject

	Class_2	Class_4	Class_6	Class_8
Sub_1	1/8	1/3/6/8	1/3/5/6/7/8	1/2/3/4/5/6/7/8
Sub_2	3/8	2/4/6/8	1/3/4/5/6/7	1/2/3/4/5/6/7/8
Sub_3	4/8	3/4/6/7	1/4/5/6/7/8	1/2/3/4/5/6/7/8
Sub_4	2/6	1/3/5/7	1/3/4/5/6/8	1/2/3/4/5/6/7/8

Compared with the binary classification results, the accuracies decreased as the number of categories increased. Notably, subject 1 showed an accuracy of 73.4% for 8 targets recognition, and almost all the subjects could achieve accuracies around or more than 70% for 4 targets recognition. The results demonstrated the effectiveness of the proposed paradigm and algorithm, while there was room for the improvement of the model.

Figure 4. Performance of the proposed BCI system.

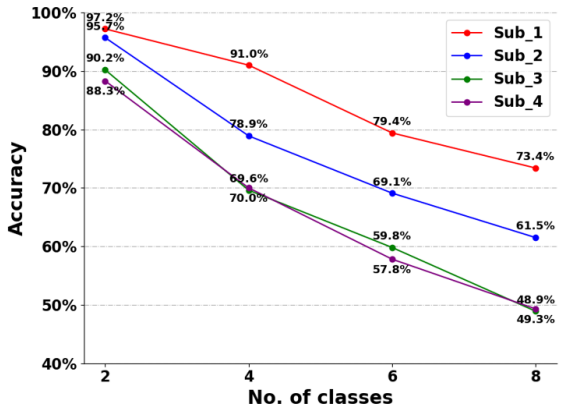

Fig. 5 shows visualizations of the relevance of each sampling point. The ordinate represents twenty-one channels, and the abscissa represents sampling points. The color represents the contribution or correlation of the sampling point to the target output node. It's obvious that the relevance maps produced by LRP for each spatial pattern were different from each other. This proved that basic graphic shapes could induce specific EEGs from the perspective of the data point relevance.

Figure 5. Visualizations of the relevance of each sampling point

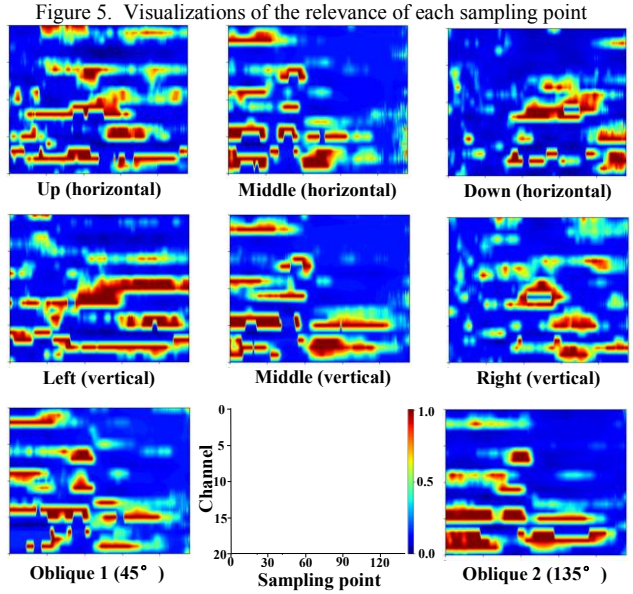

IV. Discussion and Conclusion

This study investigated the separability of EEGs induced by a same white bar with eight different spatial patterns. Eight targets were decoded through a model constructed by CNN and LSTM. The results convinced us of the recognizability of EEGs evoked by basic graphic shapes. In future work, more subjects will be recruited for results with statistical significance, and the efforts will be put into exploring the connection between the EEGs evoked by combined elements and basic elements, as well as developing more efficient deep neural networks for EEG processing. The in-depth research of EEGs evoked by basic shapes could benefit our understanding of visual neural activities and provide new coding strategies for future BCIs.

Acknowledgment

The authors sincerely thank all participants for their voluntary participation.

References

[1] J. R. Wolpaw, and E. W. Wolpaw, Brain-Computer Interfaces: Principles and Practice: Brain-Computer Interfaces: Principles and Practice, 2012.

[2] J. R. Wolpaw, N. Birbaumer, W. J. Heetderks, D. J. McFarland, P. H. Peckham, G. Schalk, E. Donchin, L. A. Quatrano, C. J. Robinson, and T. M. Vaughan, "Brain-computer interface technology: A review of the first international meeting," IEEE Transactions on Rehabilitation Engineering, vol. 8, no. 2, pp. 164-173, Jun, 2000.

[3] E. Kandel, and J. Schwartz, Principles of neural science / 5th ed: Principles of neural science / 5th ed, 2013.

[4] F. B. Vialatte, M. Maurice, J. Dauwels, and A. Cichocki, "Steady-state visually evoked potentials: Focus on essential paradigms and future perspectives," Progress in Neurobiology, vol. 90, no. 4, pp. 418-438, Apr, 2010.

[5] T. Kaufmann, and A. Kubler, "Beyond maximum speed-a novel two-stimulus paradigm for brain-computer interfaces based on event-related potentials (P300-BCI)," Journal of Neural Engineering, vol. 11, no. 5, pp. 12, Oct, 2014.

[6] Y. Miyawaki, H. Uchida, O. Yamashita, M. A. Sato, Y. Morito, H. C. Tanabe, N. Sadato, and Y. Kamitani, "Visual Image Reconstruction from Human Brain Activity using a Combination of Multiscale Local Image Decoders," Neuron, vol. 60, no. 5, pp. 915-929, Dec, 2008.

[7] T. Horikawa, and Y. Kamitani, "Generic decoding of seen and imagined objects using hierarchical visual features," Nature Communications, vol. 8, pp. 15, May, 2017.

[8] X. Zheng, W. Z. Chen, Y. You, Y. Jiang, M. Y. Li, and T. Zhang, "Ensemble deep learning for automated visual classification using EEG signals," Pattern Recognition, vol. 102, pp. 10, Jun, 2020.

[9] G. Rashkov, A. Bobe, D. Fastovets, and M. Komarova, "Natural image reconstruction from brain waves: a novel visual BCI system with native feedback," Cold Spring Harbor Laboratory, 2019.

[10] J. G. Nicholls, P. A. Fuchs, A. R. Martin, and B. G. Wallace, From Neuron to Brain: Cellular Approach to the Function of the Nervous System. Sinauer associates, 2001.

[11] O. Russakovsky, J. Deng, H. Su, J. Krause, S. Satheesh, S. Ma, Z. H. Huang, A. Karpathy, A. Khosla, M. Bernstein, A. C. Berg, and L. Fei-Fei, "ImageNet Large Scale Visual Recognition Challenge," International Journal of Computer Vision, vol. 115, no. 3, pp. 211-252, Dec, 2015.

[12] Y. M. Hou, L. Zhou, S. Y. Jia, and X. M. Lun, "A novel approach of decoding EEG four-class motor imagery tasks via scout ESI and CNN," Journal of Neural Engineering, vol. 17, no. 1, pp. 15, Feb, 2020.

[13] A. Elsheikh, S. Yacout, and M. S. Ouali, "Bidirectional handshaking LSTM for remaining useful life prediction," Neurocomputing, vol. 323, pp. 148-156, Jan, 2019.

[14] S. Hochreiter, and J. Schmidhuber, "Long short-term memory," Neural computation, vol. 9, no. 8, pp. 1735-80, 1997 Nov, 1997.

[15] L. Wilsonpauwels, E. J. Akesson, P. A. Stewart, and S. D. J. P. B. D. Spacey, "Cranial Nerves in Health and Disease," no. 4, pp. 318-318, 2002.

[16] M. P. Xu, X. L. Xiao, Y. J. Wang, H. Z. Qi, T. P. Jung, and D. Ming, "A Brain-Computer Interface Based on Miniature-Event-Related Potentials Induced by Very Small Lateral Visual Stimuli," Ieee Transactions on Biomedical Engineering, vol. 65, no. 5, pp. 1166-1175, May, 2018.